

## Porous silicon structures for low-cost diffraction-based biosensing

Judson D. Ryckman,<sup>1</sup> Marco Liscidini,<sup>2</sup> J. E. Sipe,<sup>3</sup> and S. M. Weiss<sup>1,a)</sup>

<sup>1</sup>Department of Electrical Engineering and Computer Science, Vanderbilt University, Nashville, Tennessee 37235, USA

<sup>2</sup>Dipartimento di Fisica "A. Volta," Università degli Studi di Pavia, via Bassi 6, 27100 Pavia, Italy

<sup>3</sup>Department of Physics and Institute for Optical Sciences, University of Toronto, 60 St. George St. Toronto M5S 1A7 Ontario, Canada

(Received 5 February 2010; accepted 8 April 2010; published online 28 April 2010)

We present a strategy for label-free biosensing using porous silicon diffraction gratings. The gratings are fabricated using a cost-effective, high-throughput stamping technique. Unlike traditional diffraction-based biosensors that rely on microcontact printing or lithography to create gratings for the localization of analytes on the top surface of the grating, in our structure analytes are free to infiltrate the porous network and increase the effective refractive index of the grating. The large surface area of porous silicon available for molecular binding offers the potential for enhanced diffraction response compared to nonporous gratings with limited surface area. Small molecule detection of 3-aminopropyltriethoxysilane is demonstrated. © 2010 American Institute of Physics. [doi:10.1063/1.3421545]

A growing number of optical biosensing systems rely on expensive and bulky equipment for the high resolution determination of the angle or wavelength of optical interrogation.<sup>1</sup> This limits the portability of such systems, and may restrict their usefulness in sensing applications outside of a controlled laboratory environment. Diffraction-based biosensors (DBB), on the other hand, operate at a fixed wavelength and detection angle; they exploit the variation in diffraction efficiency that occurs due to the presence of a chemical or biological species on a diffraction grating.<sup>2–4</sup> The diffraction efficiency, taken as the ratio of the output power for a selected diffraction order to the input power, is unaffected by fluctuations in the power of the probe laser.<sup>5</sup> In traditional DBBs, biochemical species are selectively adsorbed onto the top surface of a diffraction grating, giving rise to an increase in the diffraction efficiency proportional to the change in the grating thickness. Similar to other traditional biosensors, the limited surface area available for biochemical attachment on the gratings ultimately limits the device performance.

The use of porous materials with large internal surface area is a promising strategy for constructing biosensing devices.<sup>6–11</sup> Compared to many traditional sensors with limited surface area, porous sensors offer large improvements in device sensitivity, especially for small molecule detection. For example, the sensitivity and size-selectivity of traditional surface plasmon and waveguide sensors have been increased by the use of porous alumina<sup>8</sup> and porous silicon, respectively.<sup>9,10</sup> Further, porous materials can be robust, and there is often great flexibility in the design of their physical and optical properties.<sup>11</sup>

In this letter, we present a porous silicon diffraction-based biosensor (PSi-DBB) that combines the benefits of both diffraction-based biosensing and large surface area porous materials. Our PSi-DBB is a porous diffraction grating fabricated at low-cost and at high throughput by a stamping process on a PSi film. For a diffraction grating of thickness

$h$ , much smaller than the wavelength,  $\lambda$ , of the incident beam, the diffraction efficiency is<sup>12</sup>

$$\eta = \alpha(f, \Lambda, \lambda, \dots)(h\Delta n)^2, \quad (1)$$

where  $\Delta n$  is the grating refractive index contrast with respect to the cladding index, and  $\alpha$  is a coefficient that depends on the incident wavelength, the grating period  $\Lambda$ , the air filling fraction  $f$ , and the optical properties of the cladding and substrate. In traditional DBBs, analytes give rise to an increase,  $(h + \delta h)\Delta n - h\Delta n$ , in the optical thickness through an increase,  $\delta h$ , in the grating height. In a PSi-DBB, analytes infiltrate the pores and lead to a change,  $h(\Delta n + \delta\Delta n) - h\Delta n$ , in the optical thickness through a change,  $\delta\Delta n$ , in the refractive index contrast. These perturbations of the optical thickness lead to changes,  $\Delta\eta$ , in diffraction efficiency. We demonstrate the feasibility of the PSi-DBB and its potential to enhance the response of traditional DBBs, while using a simpler sample preparation protocol.

Porous silicon substrates were prepared through electrochemical etching of boron doped p+ silicon wafers ( $\langle 100 \rangle$ , 0.01–0.02  $\Omega$  cm) in a 15% ethanoic hydrofluoric acid electrolyte. A current density of 80 mA/cm<sup>2</sup> was applied for 3.5 s. Following our earlier work, we estimate that these conditions lead to a 140 nm thick film with 81% porosity.<sup>9</sup> Standard contact lithography and reactive-ion etching techniques were used to fabricate silicon grating stamps (9 mm<sup>2</sup>) composed of a 5  $\mu$ m pitch grating, 500 nm in depth. The silicon stamp was then pressed against the PSi substrate using a force of  $\approx 2000$  N to locally crush the underlying PSi layer to form a porous grating. This stamping process is notably faster and simpler than dry-removal soft lithography, which locally removes regions of weakened PSi with the use of a polydimethylsiloxane stamp.<sup>13</sup> Figure 1 reveals the imprinted PSi grating with a nominal depth of 29 nm and with a nominal air fill fraction of 0.4. It has previously been shown that the hardness of high porosity p+ PSi scales inversely with the PSi film thickness, due to the influence of the underlying substrate.<sup>14</sup> Hence, precise control over the imprinted grating height to within a few nanometers

<sup>a)</sup>Electronic mail: sharon.weiss@vanderbilt.edu.

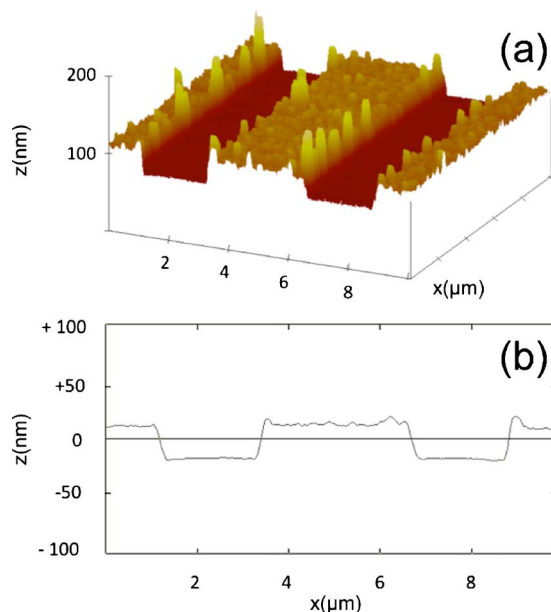


FIG. 1. (Color online) (a) Atomic force microscopy (AFM) image of the stamped porous silicon grating. (b) Cross section of the AFM profile of the porous silicon grating revealing a 29 nm grating height.

is possible by tuning the thickness of the PSi layer. Indeed, we have produced PSi-DBBs with grating heights ranging from 10–120 nm. Before stamping, samples were oxidized at 500 °C in an air ambient for 5 min in an Omegalux LMF-3550 oven. Partial oxidation of the PSi grating provides a suitable silica surface for attachment of biochemical species.<sup>15</sup> Importantly, we note that the silicon stamp can be reused multiple times without degradation. This allows for many devices to be fabricated without the need for performing repeated photolithography, making the process both cost-effective and high-throughput.

Diffraction experiments were performed with the 647 nm line from an Ar/Kr laser at an incident angle of 67° [Fig. 2]. A silicon photodetector was used to monitor the input and diffracted beam powers. An input beam power on the order of 1 mW was used in all experiments. To avoid as much scattered light as possible from the zeroth order beam, the diffracted intensity of the back diffracted  $m=-3$  diffraction order was monitored.

To demonstrate proof-of-concept behavior of the PSi-DBB, the sensor was first investigated by exposing the sample to water vapor. Before applying water vapor to the sample surface, diffraction is too weak to be observed with the camera [Fig. 3, before]. Once water vapor is applied to the sample, it condenses inside the pores and produces a

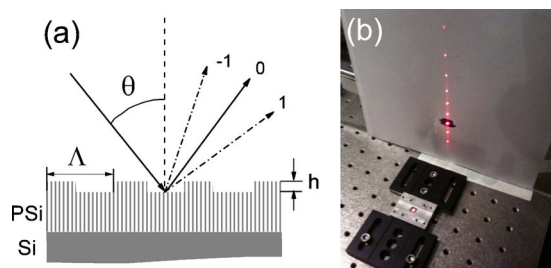


FIG. 2. (Color online) (a) Schematic of the PSi-DBB geometry. (b) Picture of the detection apparatus showing visible diffraction from a porous grating with a 60 nm grating height.

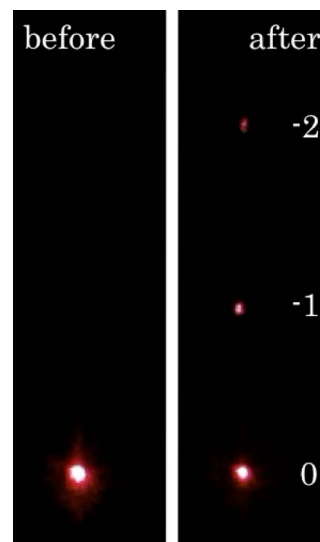


FIG. 3. (Color online) Camera images of diffraction before and after exposing the PSi-DBB to water vapor. Before exposure, the back diffracted beams  $m=-1$  and  $-2$  are too weak to be observed by the digital camera. After exposure, a large increase in diffraction efficiency is observed.

large increase in the effective refractive index of the grating due to water ( $n_{\text{water}} \approx 1.33$ ) displacing air ( $n_{\text{air}} \approx 1$ ). This increase in refractive index results in a large increase in the diffraction efficiency and the visible appearance of diffracted orders [Fig. 3, after]. We note that some scattering of specularly reflected light accompanies water vapor condensation on the sample surface and contributes to the intensity of light collected near the zeroth order beam. Within a few seconds after water vapor condensation, the water evaporates from the sample and the initial diffraction intensities are restored. The same water vapor experiment was also performed on a nonporous silicon diffraction grating of the same dimensions (not shown). In this case, no such increase to diffraction efficiency was observed. This result matches our theoretical calculations. Traditionally, DBBs rely on the adsorption of analytes to the top surface of the grating only. For our structure, condensation uniformly covered the entire nonporous grating surface, and produced no increase in optical thickness and therefore no increase in diffraction efficiency.

To demonstrate small molecule detection, we study the infiltration of 3-aminopropyltriethoxysilane (3-APTES), which is a commonly used and well-studied molecule for promoting adhesion between silica surfaces and organic materials.<sup>15</sup> PSi-DBBs are exposed to various concentrations of 3-APTES, diluted in a H<sub>2</sub>O:methanol (1:1) mixture, at varied time intervals up to 90 min. Before each measurement, the sample is rinsed vigorously in deionized water and dried under nitrogen flow to remove unbound species. Figure 4 shows the time-dependent change in diffraction efficiency  $\Delta\eta$  of the  $m=-3$  back diffracted beam over the course of the experiment for a 0.25% 3-APTES solution; the change saturates in approximately 50 min. For a 1% 3-APTES and higher concentration solutions (not shown), the diffraction efficiency saturates in under 15 min. The trend shown in Fig. 4 indicates binding of 3-APTES that is consistent with monolayer formation. Our observed saturation time for 3% 3-APTES is comparable to that observed in studies of mesoporous microcavity biosensors.<sup>16</sup> However, in the microcavity study, exposure to 0.25% 3-APTES solution led to only

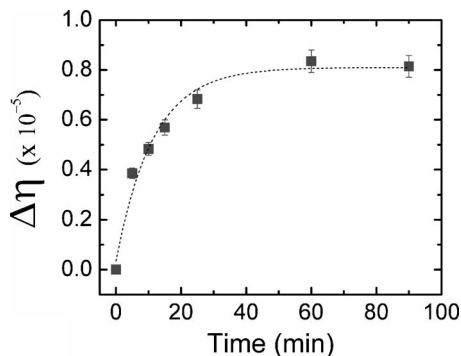


FIG. 4. Change to diffraction efficiency of the PSi-DBB during exposure to 0.25% solution of 3-APTES for grating of height  $h=29$  nm, period  $\Lambda=5$   $\mu\text{m}$ , and air fraction  $f=0.4$ . The responses are fitted with the single exponential function.

$\sim 8\%$  of a monolayer after 20 min, whereas for our structure the same exposure led to  $\sim 70\%$  of a monolayer in the same time. The distinctly faster response of our PSi-DBB is attributed to the  $\sim 30$  nm of porous grating that must be infiltrated to produce a measurable response, compared to the nearly  $2$   $\mu\text{m}$  that must be infiltrated in the microcavity sensor. Thus, the shallow geometry of our PSi-DBB favors very rapid small molecule detection.

The nominal diffraction efficiency  $\eta$  of  $m=-3$  diffraction order for the 29 nm PSi grating was  $\approx 1.7 \times 10^{-5}$  before silanization, and  $\approx 2.5 \times 10^{-5}$  after silanization, with light collected over  $\approx 1/300$  steradians. To produce a theoretical estimate of the diffraction efficiencies, we first performed reflectance measurements of uniform PSi films before and after silanization. The indices we extracted were  $n_{\text{PSi}}=1.2054$  and  $n_{\text{PSi}+3\text{-APTES}}=1.2454$ . With the nominal grating height of 29 nm and air fill fraction 0.4, a scattering matrix calculation predicts a diffraction efficiency of  $1.5 \times 10^{-5}$  before silanization and an efficiency of  $2.3 \times 10^{-5}$  after silanization.<sup>17</sup> There would be both positive and negative corrections of these ideal calculations to compare with experiment: the first because some scattered light from the specularly reflected beam arrives within the collection window, and the second because some diffracted light that would arrive within the collection window for an ideal structure is scattered out of it. Including these corrections will require further study but even at this stage we note the good qualitative agreement between theory and experiment. Furthermore, there is good quantitative agreement between theory and experiment for the change in diffraction efficiency with silanization.

In summary, we have demonstrated the fabrication and highly sensitive response of a PSi-DBB. A wide range of structures of this type can be constructed. For example, our diffraction technique could be employed in a more complicated geometry where the light-matter interaction can be enhanced through a light-confinement mechanism. Further op-

timization of the grating material, such as the incorporation of porous alumina or porous silica could be used to reduce the refractive index contrast and increase the relative change  $\Delta\eta/\eta$  in diffraction efficiency that arises in response to analyte infiltration. Our experiments and modeling suggest that the porous nature of the PSi-DBB leads to significant sensitivity improvements over traditional DBBs while maintaining the important advantages that traditional DBBs have over other detection systems as follows: (1) operation without the need for expensive and bulky equipment to perform angular or wavelength resolved measurements and (2) self-referencing. Moreover, PSi-DBBs can be fabricated in a straightforward, low-cost, and high throughput stamping process on highly tunable porous substrates.

This work was supported in part by the Army Research Office (Grant No. W911NF-09-1-0101). SEM, reflectance, and ellipsometry measurements were performed at the Vanderbilt Institute of Nanoscale Science and Engineering. Photolithography and reactive ion etching of the silicon stamps were performed at the Center for Nanophase Materials Sciences, which is sponsored at Oak Ridge National Laboratory by the Division of Scientific User Facilities, U.S. Department of Energy. The authors thank Dr. Florence Sanchez and Catherine Gay for assistance with the stamping tool. M.L. acknowledges Cnism funding through the INNESCO project. J.E.S. acknowledges support from The National Sciences and Engineering Research Council of Canada, and the Ontario Centre of Excellence program. The authors would also like to acknowledge useful discussions with Axela Inc.

<sup>1</sup>P. N. Prasad, *Introduction to Biophotonics* (Wiley, New York, 2003).

<sup>2</sup>J. B. Goh, R. W. Loo, R. A. McAloney, and M. C. Goh, *Anal. Bioanal. Chem.* **374**, 54 (2002).

<sup>3</sup>M. Liscidini and J. E. Sipe, *Appl. Phys. Lett.* **91**, 253125 (2007).

<sup>4</sup>M. Liscidini and J. E. Sipe, *J. Opt. Soc. Am.* **26**, 279 (2009).

<sup>5</sup>F. Yu and W. Knoll, *Anal. Chem.* **76**, 1971 (2004).

<sup>6</sup>F. Cunin, T. A. Schmedake, J. R. Link, Y. Y. Li, J. Koh, S. N. Bhatia, and M. J. Sailor, *Nature Mater.* **1**, 39 (2002).

<sup>7</sup>E. Guillermain, V. Lysenko, R. Orobtschouk, T. Benyattou, S. Roux, A. Pillonnet, and P. Perriat, *Appl. Phys. Lett.* **90**, 241116 (2007).

<sup>8</sup>A. G. Koutsoubas, N. Spiliopoulos, D. Anastassopoulos, A. A. Vradis, and G. D. Priftis, *J. Appl. Phys.* **103**, 094521 (2008).

<sup>9</sup>X. Wei, C. Kang, M. Liscidini, G. Rong, S. Retterer, M. Patrini, J. E. Sipe, and S. M. Weiss, *J. Appl. Phys.* **104**, 123113 (2008).

<sup>10</sup>G. Rong, J. D. Ryckman, R. Mernaugh, and S. M. Weiss, *Appl. Phys. Lett.* **93**, 161109 (2008).

<sup>11</sup>L. Pavesi, *Riv. Nuovo Cimento* **20**, 1 (1997).

<sup>12</sup>C. B. Burckhardt, *J. Opt. Soc. Am.* **57**, 601 (1967).

<sup>13</sup>D. J. Sirbully, G. M. Lowman, B. Scott, G. D. Stucky, and S. K. Buratto, *Adv. Mater.* **15**, 149 (2003).

<sup>14</sup>S. P. Duttgupta, X. L. Chen, S. A. Jenekhe, and P. M. Fauchet, *Solid State Commun.* **101**, 33 (1997).

<sup>15</sup>G. Hermanson, *Bioconjugate Techniques* (Academic, New York, 1996).

<sup>16</sup>H. Ouyang, C. C. Striemer, and P. M. Fauchet, *Appl. Phys. Lett.* **88**, 163108 (2006).

<sup>17</sup>D. M. Whittaker and I. S. Culshaw, *Phys. Rev. B* **60**, 2610 (1999).